IET Radar, Sonar & Navigation

Research Article

IET Journals
The Institution of Engineering and Technology

Impact quantification of satellite outages on air navigation continuity

ISSN 1751-8784
Received on 15th August 2018
Accepted on 18th October 2018
doi: 10.1049/iet-rsn.2018.5376
www.ietdl.org

Yawei Zhai[1] ✉, Xingqun Zhan[1], Mathieu Joerger[2], Boris Pervan[3]

[1]*School of Aeronautics and Astronautics, Shanghai Jiao Tong University, 800 Dongchuan Rd., Shanghai, People's Republic of China*
[2]*Department of Aerospace and Mechanical Engineering, The University of Arizona, 1130 N. Mountain Ave., Tucson, USA*
[3]*Mechanical, Materials and Aerospace Engineering, Illinois Institute of Technology, 10 West 32nd St., Chicago, USA*
✉ *E-mail: yawei.zhai@sjtu.edu.cn*

Abstract: Advanced receiver autonomous integrity monitoring (ARAIM) using multiple global navigation satellite system constellations is expected to bring significant navigation performance improvement to civil aviation. However, using multiple constellations, the higher number of satellite outages due, for example, to routine station keeping manoeuvres, could significantly increase continuity risk. In response, this study proposes a new method to rigorously quantify the impact of satellite outages on navigation safety. To achieve this, integrity and continuity risk bounds are derived, which account for all possible outage conditions. In addition, the proposed approach allows to determine whether an exclusion function is needed following an outage event. The method is implemented to analyse horizontal ARAIM (H-ARAIM) availability performance. Results indicate that dual-constellation H-ARAIM can provide high service availability, where both integrity and continuity requirements are met.

1 Introduction

Global navigation satellite systems (GNSS) measurements are vulnerable to faults including satellite and constellation failures [1], which can potentially lead to catastrophic consequences in safety-critical applications. To mitigate their impact, receiver autonomous integrity monitoring (RAIM) has been used in aviation as a backup navigation tool [2–4]. The core principle of RAIM is to exploit redundant measurements to achieve self-contained fault detection (FD) at the user receiver [5]. Future GNSS constellations will provide dramatically increased measurement redundancy and reduced measurement errors. These developments, together with advances in the RAIM concept itself, will open the possibility to independently support aircraft navigation using GNSS during all phases of flight (from take-off, through en-route flight, and final approach to landing) with minimal investment in ground infrastructure. Therefore, considerable effort has recently been expended, especially in the European Union and the USA, to develop new dual-frequency, multi-constellation advanced RAIM (ARAIM) FD and exclusion (FDE) methods [6–8].

Currently, two versions of ARAIM, corresponding to two operational scenarios, are being investigated [9]. Horizontal ARAIM (H-ARAIM) mainly aims at providing horizontal navigation integrity for aircraft en-route flight. Vertical ARAIM (V-ARAIM) is intended for localiser performance with vertical guidance (LPV) with the goal of leading the aircraft to a 200-foot decision height; this operation is called LPV-200. In comparison with H-ARAIM, V-ARAIM integrity requirements are more stringent because the alert limits (AL) for LPV-200 are significantly smaller than for H-ARAIM operations. However, the continuity requirements for H-ARAIM are more stringent than for V-ARAIM. This is because when losing navigation continuity during an approach, the aircraft can switch to a different operational mode, e.g. abort landing, go around, and try an approach again. Those manoeuvres are not unusual during landing and do not impact operational safety [10]. In contrast, H-ARAIM missions cannot easily be aborted once started, and alternative navigation methods must be found when loss of continuity (LOC) occurs. When ARAIM is used as primary navigation system, LOC during operation can lead the aircraft to be left without a means of navigation, which is highly undesirable. This work focuses on ensuring H-ARAIM continuity. The proposed methods also apply to V-ARAIM.

As an evolution of RAIM, H-ARAIM will take advantage of GNSS modernisation and of newly deployed GNSS. In particular, the role transition from backup to primary means of navigation has increased the significance of H-ARAIM continuity as compared to conventional RAIM. Most prior ARAIM work focused on reducing integrity risk [11–13]. Only few investigated continuity, and in most cases, false alarm (FA) was considered the only source of LOC [14, 15]. However, to properly evaluate the overall continuity risk, all sources of LOC must be accounted for. Causes of LOC include FD, satellite outages (SO), ionospheric scintillation (IOSC), and radio frequency interference (RFI) [16]. When using multiple GNSS constellations in ARAIM, the heightened likelihood of satellite fault and SO can impact navigation continuity [17]. Moreover, satellite failure and outage rates may be larger in newly deployed constellations, which could further decrease navigation continuity.

To reduce the continuity risk caused by frequent FD, a fault exclusion method was proposed in our prior work [18]. An exclusion function is executed after a fault is detected, and it autonomously identifies and removes the cause of the alarm, thereby preserving navigation continuity. To assess the impact of unscheduled SO (USO) on continuity, we employed a 'critical satellite' approach described in [17, 19]. However, evaluating the number of critical satellites requires a separate, computationally-expensive analysis. This is not a problem for ground-based augmentation system operations, because the evaluation is performed at the ground [20]. However, an airborne ARAIM receiver cannot handle such computational complexity. In addition, the integrity risk equations that define critical satellites can be overly conservative [17]. In response, this paper develops new methods to quantify the impact of SO on H-ARAIM continuity. The key contribution is a rigorous derivation of a continuity risk equation that accounts for LOC contributions from both measurement faults and outages. This new approach incorporates the separate critical satellite analysis into a single integrity risk equation, which can then be applied for ARAIM service availability prediction.

Section 2 of this paper gives an overview of the real-time ARAIM FDE user algorithm. The test statistics are defined, practical implementation procedures are detailed, and the integrity risk is bounded. The methods derived in later sections are all based on this algorithm.

In Section 3, the impact of SO on continuity is discussed, and the overall ARAIM continuity risk equation is derived. The

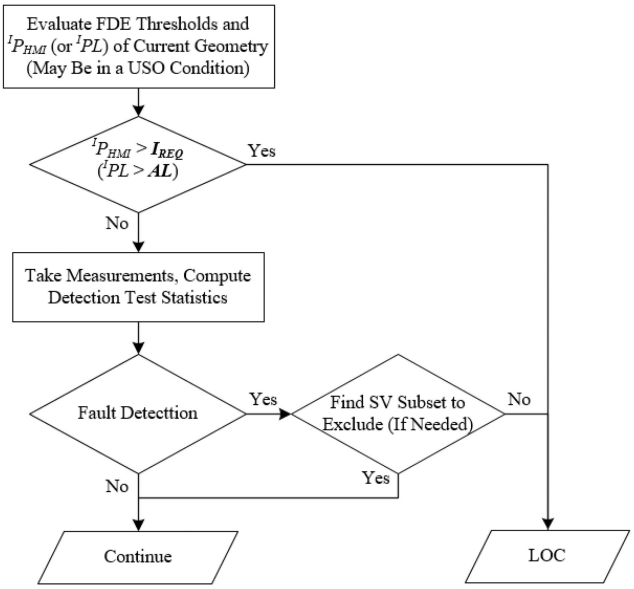

Fig. 1 *Flow diagram of the real-time FDE process*

equation accounts for all SO scenarios and for all fault modes. The LOC contributions from those events can be controlled by setting FDE thresholds. Other LOC sources, such as IOSC and RFI, are treated together by allocating a continuity budget.

Section 4 describes two approaches to evaluate the FDE thresholds, using equally allocated continuity budgets over SO scenarios and using a more advanced method. First, the equal-allocation approach can be carried out without the receiver having to recognise whether a SO is actually present, and the values assigned for threshold computation are independent of the current SO condition. Then, since SO status can actually be determined at the airborne receiver, different continuity budgets can be applied for those cases. This second approach can result in smaller integrity risk contributions, and allows to identify whether an exclusion function is needed or not after an outage has occurred.

Finally, the last section of this paper presents an overall H-ARAIM navigation availability performance. The predictive integrity risk bound is derived by weighting the instantaneous integrity risk using SO prior probabilities. It characterises both SO and faults. Required navigation performance (RNP) 0.1 and 0.3 are used as example operations to show the achievable H-ARAIM performance (RNP 0.1 is the most stringent navigation requirement for H-ARAIM operations.). For a baseline GPS/Galileo constellation, the two continuity risk allocation approaches are analysed, both of which achieve high service availability.

2 ARAIM FDE algorithm

To improve navigation continuity, we designed a solution separation (SS) based fault exclusion algorithm [18]. This section describes the implementation of this algorithm, and derives integrity risk bounds for both FD-only and FDE. For analysis purposes, two types of integrity risk are introduced in this paper. First, instantaneous integrity risk, $^{I}P_{\mathrm{HMI}}$, refers to the one computed at the receiver in real time using the current satellite geometry. The left superscript 'I' denotes 'instantaneous', and the details of computing $^{I}P_{\mathrm{HMI}}$ will be provided later in Section 2.2. Then, predictive integrity risk, $^{P}P_{\mathrm{HMI}}$, is evaluated on the ground to analyse and predict ARAIM continuity and coverage performance. The left superscript 'P' of $^{P}P_{\mathrm{HMI}}$ refers to 'predictive' and more details will be provided in Section 5. It is noteworthy that the airborne user receiver may have been experiencing SO during operation, so $^{I}P_{\mathrm{HMI}}$ is conditioned on the presence of the SO. But to lighten notations, in this section, no specific subscript is employed to identify the SO condition. Those notations are introduced in later sections to quantify the overall continuity risk.

2.1 Real-time FDE process

Prior work assessing the need of ARAIM fault exclusion [18] showed that an airborne H-ARAIM exclusion function is always required to meet continuity requirements. In contrast, V-ARAIM exclusion may only be needed if four constellations are used or/and if the constellations have large fault probabilities. This work focuses on H-ARAIM. The need of H-ARAIM exclusion is reassessed in this paper after we derive a new continuity equation that captures LOC due to SO.

Fig. 1 is a flow diagram that summarises the real-time ARAIM FDE procedure. It starts with evaluating the instantaneous integrity risk $^{I}P_{\mathrm{HMI}}$, or instantaneous protection level ($^{I}\mathrm{PL}$), using the current visible geometry. The remaining FDE steps will be implemented only if the integrity risk requirement I_{REQ} or AL of the intended operation is met. For continuity, the key element is the exclusion step following detection, and the mechanism to determine which space vehicles (SVs) to exclude, both of which will be described hereafter. For H-ARAIM, the probability of GPS constellation fault is assumed to be 10^{-8} [21], so GPS can be relied upon to exclude other constellation faults even in the dual-constellation case.

A baseline multiple hypotheses SS ARAIM detection algorithm is described in [5, 8]. Using similar notations as our previous work [18, 22], the normalised detection test statistics q_d can be expressed as

$$q_d = \frac{\hat{x}_0 - \hat{x}_d}{\sigma_{\Delta_d}} = \frac{\varepsilon_0 - \varepsilon_d}{\sigma_{\Delta_d}}, \quad \text{for } d = 1 \ldots h. \tag{1}$$

where $\hat{x}_0$ is the least squares scalar position estimate using all satellites in view, for a position coordinate of interest (e.g. for the east and/or north direction in H-ARAIM); $\hat{x}_d$ is the least squares position estimate using all satellites except the one(s) included in fault mode d, $d = 1, \ldots h$; h is the number of fault modes that need to be monitored; σ_{Δ_d} is the standard deviation of the SS detection statistic Δ_d, which is defined as the difference between $\hat{x}_0$ and $\hat{x}_d$; ε_0 is the position estimate error of $\hat{x}_0$, having a normal distribution with standard deviation σ_0 and with a mean's absolute value no greater than b_0; and ε_d is the position estimate error of $\hat{x}_d$, following a normal distribution with bounding bias b_d and standard deviation σ_d.

In the detection step, the statistics in (1) are compared with their corresponding thresholds T_d, which are derived in Section 4 to achieve an allocated FA budget. If any of the statistics exceeds its threshold, i.e. if $\cup_{d=1}^{h} |q_d| > T_d$, then an alert is issued, indicating that a fault may be present: this event is labelled D_0. Otherwise, if all test statistics are smaller than their corresponding thresholds, i.e. if $\cap_{d=1}^{h} |q_d| < T_d$, then there is no detection (event $\bar{D}_0$), and the operation continues.

If an exclusion function is implemented, it is executed after an alert occurs. In our design, the exclusion function is a two-step process. The first step aims at prioritising exclusion options considering the set of statistics q_d arranged in descending magnitude. This approach is employed because each q_d is tailored to a specific fault mode, and the most likely fault hypothesis is the one corresponding to the maximum q_d. The purpose of this first step is to speed up the exclusion decision. As measurements are noisy, there will be cases when the maximum statistic does not correspond to the actual fault mode. That is why a second step must be applied.

In the second step, the exclusion option is validated. The second layer of detection tests is employed to confirm that the remaining satellite subset is fault free. The normalised exclusion statistics (i.e. the second layer detection statistics) are defined as

$$q_{e,l} = \frac{\hat{x}_e - \hat{x}_{e,l}}{\sigma_{\Delta_{e,l}}} = \frac{\varepsilon_e - \varepsilon_{e,l}}{\sigma_{\Delta_{e,l}}} \quad \text{, for } l = 1 \ldots s. \tag{2}$$

where $\hat{x}_e$ is the least squares position estimate using the remaining satellites after excluding subset e, $e = 1, \ldots h$ (which includes all

faulted SVs under fault mode e); $\hat{x}_{e,l}$ is the least squares position estimate using satellites remaining after excluding subset e, and after also excluding possibly faulted satellites under the second layer of fault modes l, $l = 1, \ldots s$; $\sigma_{\Delta_{e,l}}$ is the standard deviation of the exclusion statistic $\Delta_{e,l}$, which is defined as the difference between $\hat{x}_e$ and $\hat{x}_{e,l}$; and $\varepsilon_{e,l}$ is the position estimate error of $\hat{x}_{e,l}$, having a normal distribution with bounding bias $b_{e,l}$ and standard deviation $\sigma_{e,l}$.

This second step considers all exclusion options following the order determined in step 1. For each option, the exclusion test compares each $q_{e,l}$ with its associated threshold $T_{e,l}$, which is also derived in Section 4 using the allocated continuity budget. If all the exclusion statistics are within their thresholds, i.e. if $\cap_{l=1}^{s} |q_{e,l}| < T_{e,l}$, then the associated SV subset is chosen to be excluded.

It is possible that no exclusion (NE) is validated, even after testing all options. This event can be expressed as: $\cap_{e=1}^{h} \{ \cup_{l=1}^{s} |q_{e,l}| > T_{e,l} \}$. This case results in LOC, and its probability of occurrence will be evaluated in Section 3. Thus, after detection, two conditions are necessary for a satellite subset j to be excluded (this event is noted E_j): (i) no alert is triggered by the second layer of detection, after excluding subset j (event $\bar{D}_j$); (ii) the detection statistic q_j corresponding to subset j is the largest among the subsets that pass the exclusion test (event MAX_j).

2.2 Instantaneous integrity risk

Integrity is a measure of the trust that can be placed in the correctness of the information supplied by the total navigation system [10]. Integrity risk is defined as the probability that an undetected navigation error results in hazardous misleading information (HMI). HMI occurs when the position error exceeds a predefined AL and no alert is given. As H-ARAIM only provides horizontal navigation service, only the horizontal AL (HAL) needs to be considered. As shown in Fig. 1, for a-priori integrity risk evaluation, the receiver does not know whether a fault will be detected or not, and it does not know which satellite subset will be excluded. Therefore, all possible integrity threats are considered.

Using FD-only, no integrity risk other than missed detection affects the system. So, the integrity risk under FD-only is a joint probability of having a hazard and sending no alert ($\bar{D}_0$) [5]

$$ {}^{\mathrm{I}}P_{\mathrm{HMI,FD}} = P\left(HI_0,\ \bar{D}_0\right) \tag{3} $$

where HI_0 represents the event of hazardous information existing in the full-set solution, i.e. $|\varepsilon_0| > \ell$, where ℓ is the AL; $\bar{D}_0$ is the event of no FD using all satellites in view. Considering multiple mutually-exclusive, exhaustive fault hypotheses, (3) can be rewritten as and bounded by [5, 22]

$$ {}^{\mathrm{I}}P_{\mathrm{HMI,FD}} = \sum_{i=0}^{H} P\left(|\varepsilon_0| > \ell,\ \bigcap_{d=1}^{h} |q_d| < T_d \,\middle|\, H_i \right) P_{H_i} \tag{4} $$

$$ \begin{aligned} &< P(|\varepsilon_0| > \ell \,|H_0) P_{H_0} \\ &\quad + \sum_{i=1}^{h} P\left(|\varepsilon_i| + T_i \sigma_{\Delta_i} > \ell \,\middle|\, H_i\right) P_{H_i} + P_{\mathrm{NM,Fault}} \end{aligned} \tag{5} $$

In (4), H_i denotes the fault hypotheses for $i = 0, 1, \ldots, H$, which account for all faulty SV combinations of the measurements including fault free (FF), single satellite fault, multiple satellite faults, constellation fault. H is greater than h. P_{H_i} is the prior probability of occurrence of H_i, which is derived from the prior probabilities of satellite fault P_{sat} and constellation fault P_{const}. To avoid confusion, it is worth clarifying that the subscript '0' of H_0 indicates the FF state, whereas the '0' of D_0 and $\bar{D}_0$ represent the use of all-in-view satellites. The third term of (5), $P_{\mathrm{NM,Fault}}$, denotes the summation of prior probabilities for all non-monitored fault modes [5, 22].

If an airborne exclusion function is implemented, the integrity risk equation becomes [18]

$$ {}^{\mathrm{I}}P_{\mathrm{HMI,FDE}} = P\left(HI_0,\ \bar{D}_0\right) + \sum_{j=1}^{h} P\left(HI_j,\ E_j,\ D_0\right) \tag{6} $$

where HI_j is the event that hazardous information exists in a subset solution after excluding faulted SV(s) under fault mode j, i.e. $|\varepsilon_j| > \ell$. As compared with (3), the additional term in (6) captures the risk of wrong exclusions, which is the cost of employing an exclusion function to improve continuity. That is, the user may still be in a hazardous state even if a fault is detected and measurements excluded. To evaluate ${}^{\mathrm{I}}P_{\mathrm{HMI,FDE}}$, an upper bound is derived in [18], and the final expression is given as

$$ \begin{aligned} {}^{\mathrm{I}}P_{\mathrm{HMI,FDE}} &< P(|\varepsilon_0| > \ell \,|H_0) P_{H_0} + \sum_{i=1}^{h} P\left(|\varepsilon_i| + T_d\, \sigma_{\Delta_d} > \ell \,\middle|\, H_i\right) P_{H_i} \\ &+ \sum_{j=1}^{h} \left(\begin{array}{c} P(|\varepsilon_j| > \ell \,|H_0) P_{H_0} + \sum_{\substack{i=1 \\ S_i \subseteq S_j}}^{h} P\left(|\varepsilon_j| > \ell \,|H_i\right) P_{H_i} \\ + \sum_{\substack{i=1 \\ S_i \not\subset S_j}}^{h} P\left(|\varepsilon_{j,i}| + T_{j,i}\, \sigma_{\Delta_{j,i}} > \ell \,|H_i\right) P_{H_i} \end{array} \right) + P_{\mathrm{NM,Fault}} \end{aligned} \tag{7} $$

3 Overall continuity risk

In aviation navigation, continuity measures the capability of the system to perform its function without unscheduled interruptions during the intended operation. The continuity risk, or probability of LOC P_{LOC}, is the probability of a detected but unscheduled navigation function interruption after an operation has been initiated [10]. For H-ARAIM, the occurrence of LOC is considered a minor severity event [23].

The International Civil Aviation Organisation (ICAO) specifies the continuity risk requirement C_{REQ} for H-ARAIM operations in the range of 10^{-8}–10^{-4}/h. The existence of a range, rather than a single value, accounts for the number of aircraft that are simultaneously using the same navigation service. According to [10], the navigation system continuity requirement C_{REQ} for a single aircraft is 10^{-4}/h. However, this requirement is flexible for satellite-based systems, depending on traffic density and airspace complexity. For example, the most stringent requirement of 10^{-8}/h is suitable for areas where many aircrafts use the same service and where additional navigation tools are unavailable. The intermediate value of 10^{-6}/h can be used for situations of high air traffic density and airspace complexity, but other means to mitigate LOC are available. Specifications for C_{REQ} vary with aircraft operation. For example, [24] specifies that C_{REQ} for en-route flight is 10^{-5} and 10^{-6}/h for lateral navigation only approach; [25] uses a different range for the continuity risk requirement from 10^{-7} to 10^{-5}/h. For simulation purposes, a C_{REQ}-value of 10^{-6}/h is selected. This value is consistent with ICAO specifications, considering that backup navigation equipment is mandatory for civilian commercial aircraft. It implies that 100 aircrafts can simultaneously use the same GNSS navigation service in a same region of operation [26], and that possible LOC-mitigation means are available.

3.1 Satellite outages

SO is a major source of LOC in H-ARAIM because SV losses can significantly weaken satellite geometry. SO can be classified into two types: scheduled SO (SSO) are usually planned for satellite maintenance, and they are announced at least 48 h in advance to the user; USO are typically caused by sudden system malfunctions [27]. H-ARAIM assumes that no ARAIM-specific information is provided to the receiver at dispatch [23]. Therefore, SSO are treated as a source of H-ARAIM LOC, just as USO are.

To quantitatively capture the P_{LOC} contribution due to SO, a SO model must be considered. For the GPS constellation, the GPS standard positioning service performance standard (GPS SPS PS) has committed to a USO occurrence rate of $<2 \times 10^{-4}$/h/SV [27]. The actual USO rate was evaluated in prior work [28] by processing GPS data from January 1999 through August 2011. The actual USO rate over that period was 6.67×10^{-5}/h/SV, which is well below the GPS commitment. A more recent study from Stanford University reveals that the total SO rate from 2012 to 2016, including both SSO and USO, is 1.28×10^{-4}/h/SV [29]. For continuity evaluation, ARAIM considers historical constellation performance when it is available [16]. This paper assumes an example value for the SO probability, P_{out}, of 2×10^{-4}/h/SV. The same P_{out}-value is assumed for all constellations.

3.2 Quantifying H-ARAIM continuity risk

To evaluate the probability of LOC (P_{LOC}), all sources of LOC must be accounted for, including FA, FD, SO, IOSC, RFI, and so on. The continuity risk contributions can be classified in two categories:

$$P_{LOC} = P_{alert} + P_{other} \tag{8}$$

In (8), P_{alert} is the probability of the airborne receiver issuing an alert, which can happen under two scenarios: using FD-only if true or false detection occurs, or using FDE if detection occurs but NE option is validated. P_{alert} is used to set detection and exclusion thresholds. Other than airborne alerts, all cases of ${}^{I}P_{HMI}$ exceeding the integrity risk requirement I_{REQ} are perceived at the receiver as sources of LOC, and are grouped together under P_{other}. Root causes for ${}^{I}P_{HMI} > I_{REQ}$ include poor satellite geometries, e.g. due to SO, which we will analyse in Section 5. Other root causes that are not as well understood as SO include unusually high σ_{URA} or b_{nom}, IOSC, RFI, and so on. Evaluating the impact of these other root causes on LOC requires separate analyses, which are beyond the scope of this work. Instead, we will assign a continuity budget to account for those events and assume their continuity risk contributions are always below the budget. As an example in this work, C_{REQ} is evenly allocated so that the requirements for P_{alert} (i.e. $P_{alert,REQ}$) and for P_{other} (i.e. $P_{other,REQ}$) are both equal to 5×10^{-7}/h.

Using FDE, events of detection with NE result in alerts. Considering a set of mutually exclusive, exhaustive SO conditions, P_{alert} can be expressed as

$$P_{alert} = \sum_{k=0}^{N} P(D_k,\ \bar{E}_k | O_k) P_{O_k} \tag{9}$$

where O_k designates the SO hypothesis for satellite subset $k = 0, 1, \ldots N$, and N is the total number of possible SO hypotheses. SO combinations include the outage-free (OF) condition noted O_0, single SO, dual SO, and so on. Unlike the satellite failure model, there is no common cause to result in a constellation outage. So N only accounts for SO, whereas H in (4) combines satellite and constellation fault hypotheses. P_{O_k} is the prior probability of occurrence of event 'O_k', which can be derived from P_{out} [17]. D_k indicates that detection occurs using SVs available under 'O_k', and '$k = 0$' denotes that all SVs are available. The event $\bar{E}_k$ means that NE was achieved under 'O_k'.

Considering all fault hypotheses under each SO scenario, (9) becomes

$$P_{alert} = \sum_{k=0}^{N} \left(\sum_{i=0}^{H_k} P(D_k,\ \bar{E}_k | H_i,\ O_k) P_{H_i} \right) P_{O_k} \tag{10}$$

In (10), the total number of fault hypotheses may vary under different outage cases 'O_k', and is noted 'H_k' instead of 'H' in (4). This modification applies to all notations in the rest of the paper: 'h' becomes 'h_k', 's' becomes 's_k', and so on. Equation (10) can be rewritten as

$$P_{alert} = \sum_{k=0}^{N} \left(\begin{array}{c} P(D_k,\ \bar{E}_k | H_0,\ O_k) P_{H_0} \\ + \sum_{i=1}^{H_k} P(D_k, \bar{E}_k | H_i, O_k) P_{H_i} \end{array} \right) P_{O_k} \tag{11}$$

All the contributions to P_{alert} are captured in (11). Fig. 2 shows an H-ARAIM continuity tree that captures those contributions. Under fault-free conditions ($i = 0$), the probability of having a FA but NE event (P_{FANE}) can be limited by setting detection thresholds. In the presence of a fault ($i \neq 0$), the probability of FD but NE (P_{FDNE}) can be controlled by setting the exclusion thresholds. These points are discussed in Section 4.

4 Evaluating FDE threshold

The joint event of FD and NE in (11) can be expressed in mathematical terms using detection and exclusion test statistics described in Section 2. This will be relevant in this section for threshold setting because the test statistic distributions are known and fully defined. In this section, we present two ways to allocate $P_{alert,REQ}$: considering equal budget allocation for FANE and FDNE under all 'O_k' events, or considering a more advanced allocation.

4.1 Equal allocation over SO conditions

Equation (11) can be further bounded considering the following inequality:

$$P_{alert} < \sum_{k=0}^{N} \left(\begin{array}{c} P(D_k | H_0,\ O_k) P_{H_0} \\ + \sum_{i=1}^{h_k} P(\bar{E}_k | H_i, O_k) P_{H_i} + P_{NM,Fault} \end{array} \right) P_{O_k} \tag{12}$$

In (12), h_k denotes the total number of monitored fault hypotheses under SO condition 'O_k'. The first two terms inside the parenthesis, respectively, bound the FANE and FDNE events [18]. As P_{O_k} over all SO events sums up to 1, $P_{alert,REQ}$ will be met if the summation inside the parenthesis is ensured to be less than $P_{alert,REQ}$. Therefore, $P_{alert,REQ}$ is further allocated to account for the three terms in (12). An example allocation used in Section 5 is listed in Table 1.

Using this approach, the allocated values in Table 1 are independent of the SO scenario. Therefore, regardless of which SV(s) is out, a single $P_{FANE,REQ}$-value is needed to compute the detection threshold, and a single $P_{FDNE,REQ}$-value is used to compute the exclusion threshold. According to our prior work in [17], FDE thresholds can be evaluated using the following equations:

$$T_d = Q^{-1}\left\{ \frac{P_{FANE,REQ}}{2 P_{H_0} \cdot h_k} \right\} \tag{13}$$

$$T_{i,l} = Q^{-1}\left\{ \frac{P_{FDNE,REQ}}{2 P_{H_i} \cdot h_k \cdot s_k} \right\} \tag{14}$$

where T_d are detection thresholds for $d = 1, \ldots h$, $T_{i,l}$ are exclusion thresholds for $i = 1, \ldots h$, $l = 1, \ldots h_i$, and $Q^{-1}\{\cdot\}$ is the inverse tail probability function of the standard normal distribution.

By allocating the same continuity budget to FANE and FDNE events over all SO conditions, (13) and (14) can directly be applied to compute FDE thresholds. This approach does not require the user to monitor the presence of SO. However, this allocation may result in a large predictive integrity risk because FDE thresholds under SO condition are as large as the ones under OF condition. The next approach accounts for prior probabilities P_{O_k} in continuity risk requirement allocation for threshold evaluation.

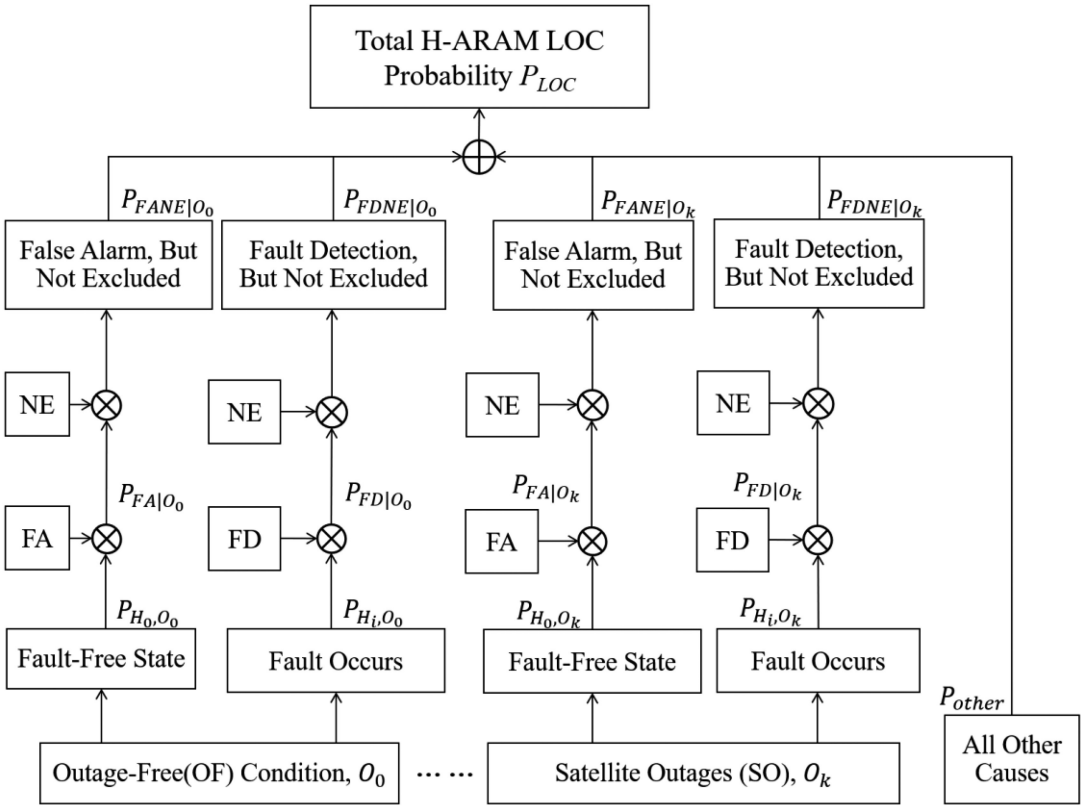

Fig. 2 *H-ARAIM LOC tree*

Table 1 H-ARAIM $P_{\text{alert, REQ}}$ allocation (independent with SO)

LOC categories	Allocated budget
$P_{\text{FANE, REQ}}$	2×10^{-7}/h
$P_{\text{FDNE, REQ}}$	2×10^{-7}/h
$P_{\text{NM, Fault, REQ}}$	10^{-7}/h

Table 2 H-ARAIM $P_{\text{alert, REQ}}$ allocation (dependent on SO)

LOC categories	Allocated budget
$P_{\text{FANE, OF, REQ}}$	10^{-7}/h
$P_{\text{FDNE, OF, REQ}}$	2×10^{-7}/h
$P_{\text{FANE, SO, REQ}}$	10^{-7}/h
$P_{\text{FDNE, SO, REQ}}$	10^{-7}/h

4.2 Non-equal allocation over SO conditions

The allocated continuity budget can be modified to account for the fact that the user knows when a SO is occurring. The total budget $P_{\text{alert, REQ}}$ can be optimally allocated to adjust the tightness of the FDE thresholds among events 'O_k', which directly impacts the contribution to integrity risk. The optimisation process is not the focus of this paper, so it is not described in detail. Instead, an example allocation is presented to illustrate the idea, and to make comparisons with the above equal-allocation approach.

The FANE and FDNE events in (11) are, respectively, expressed under OF ($k = 0$) and SO ($k \neq 0$) conditions. Therefore

$$P_{\text{alert}} = P_{\text{FANE, OF}} + P_{\text{FDNE, OF}} + P_{\text{FANE, SO}} + P_{\text{FDNE, SO}} \quad (15)$$

Table 2 lists example requirement allocations for all four terms in (15). FDE thresholds can be obtained by constraining each term to be smaller than its allocated requirement. These terms are bounded using the following inequalities, and the derivations for evaluating the thresholds are provided in Appendix.

The first term on the right side of (15), $P_{\text{FANE, OF}}$, can be bounded as

$$P_{\text{FANE, OF}} < P(D_0|H_0, O_0)P_{H_0}P_{O_0} \quad (16)$$

and the detection threshold under OF condition ($T_{d|O_0}$) is

$$T_{d|O_0} = Q^{-1}\left\{\frac{P_{\text{FANE, OF, REQ}}}{2P_{H_0} \cdot P_{O_0} \cdot h_0}\right\} \quad (17)$$

The second term on the right side of (15), $P_{\text{FDNE, OF}}$, can be bounded as

$$P_{\text{FDNE, OF}} < \sum_{i=1}^{H_0} P(\bar{E}_0|H_i, O_0)P_{H_i}P_{O_0} \quad (18)$$

and the exclusion threshold under OF condition ($T_{i,l\,|O_0}$) is

$$T_{i,l\,|O_0} = Q^{-1}\left\{\frac{P_{\text{FDNE, OF, REQ}} - P_{\text{NM, Fault}}P_{O_0}}{2P_{H_i} \cdot P_{O_0} \cdot h_0 \cdot s_0}\right\} \quad (19)$$

The third term on the right side of (15), $P_{\text{FANE, SO}}$, can be bounded as

$$P_{\text{FANE, SO}} < \sum_{k=1}^{N} P(D_k|H_0, O_k)P_{H_0}P_{O_k} \quad (20)$$

and the detection threshold under SO condition ($T_{d|O_k}$) is

$$T_{d\,|O_k} = Q^{-1}\left\{\frac{P_{\text{FANE, SO, REQ}} - P_{H_0}P_{\text{NM, SO}}}{2P_{H_0} \cdot P_{O_k} \cdot n \cdot h_k}\right\} \quad (21)$$

where $P_{\text{NM, SO}}$ is similar to $P_{\text{NM, Fault}}$, which accounts for the probability of multiple simultaneously occurring SO; these separate cases of multiple simultaneously occurring SO are considered such

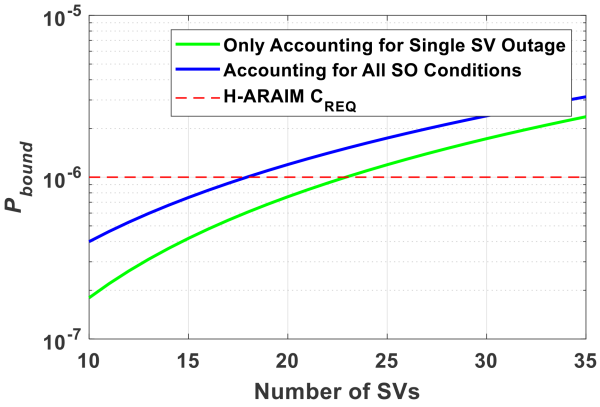

Fig. 3 *P_{bound} as a function of the SV number*

Table 3 H-ARAIM simulation scenarios

Scenarios	Values
constellations	24 GPS + 24 Galileo
error model	nominal model described in [9]
mask angle	5°
user grid	latitude by longitude: 10° × 10°
simulation time period	1 day
time steps	10 min
I_{REQ}	10^{-7}/h
C_{REQ}	10^{-6}/h
HAL	RNP 0.1: 0.1 nm (185 m) RNP 0.3: 0.3 nm (556 m)
P_{sat}	10^{-5}
P_{const}	GPS: 10^{-8}/Galileo: 10^{-4}
P_{out}	2×10^{-4}
σ_{URA}	2.4 m
σ_{URE}	2/3 σ_{URA}
b_{nom}	0.75 m
coverage range	worldwide

that $P_{NM,SO} \ll P_{FANE,SO,REQ}$. The fourth term on the right side of (15), $P_{FDNE,SO}$, can be bounded as

$$P_{FDNE,SO} < \sum_{k=1}^{N} \left\{ \sum_{i=1}^{H_k} P(\bar{E}_k | H_i, O_k) P_{H_i} \right\} P_{O_k} \tag{22}$$

and the exclusion threshold under SO condition ($T_{i,l|O_k}$) is

$$T_{i,l|O_k} = Q^{-1}\left\{ \frac{P_{FDNE,SO,REQ} - P_{NM,Fault} P_{NM,SO}}{2 P_{H_i} \cdot P_{O_k} \cdot n \cdot h_k \cdot s_k} \right\} \tag{23}$$

It is worth noting that, in (22), the sum of products of prior probabilities of faults and SO is generally very small. Bounding the inner term $P(\bar{E}_k | H_i, O_k)$ by 1, (22) can be further upper bounded using the following inequality:

$$P_{FDNE,SO} < \sum_{k=1}^{N} \sum_{i=1}^{H_k} P_{H_i} P_{O_k} \equiv P_{bound} \tag{24}$$

If P_{bound} is smaller than $P_{FDNE,SO,REQ}$, the continuity requirement can be met without performing the exclusion function. Therefore, if a SO occurs, the user receiver only needs to implement the FD function.

Fig. 3 shows P_{bound} as a function of the number of SVs in view. The blue and green lines, respectively, represent the case of accounting for all SO conditions versus considering single SV outages only. Conservative values, which are typically used for integrity evaluation ($P_{out} = 2 \times 10^{-4}$, $P_{sat} = 10^{-5}$ and $P_{const} = 10^{-4}$) [21], are used in Fig. 3. When the two solid lines exceed the requirement $P_{FDNE,SO,REQ}$, the exclusion function is needed after a SO occurs. But operationally, the risk of LOC may be acceptable even without exclusion because the lines never significantly exceed the allocated requirement. This is especially true given that less conservative fault and SO probabilities – for example, based on historical data – may be used when computing continuity risk.

Since the last two components of (15) include SO prior probabilities, the resulting FDE thresholds in (21) and (23) can be set much tighter than the ones under OF condition, i.e. (17) and (19). Therefore, their corresponding contributions to the predictive integrity risk can be significantly reduced. However, comparing to the equal allocation approach, the thresholds in (17)–(23) are all dependent on the presence of the SO. Therefore, this approach requires that the receiver continuously monitors the SO status during flight. There are operational challenges in determining a SO condition at the starting point of the operation, in distinguishing SO from other potential causes of temporary signal loss, and in identifying times where a satellite that was out is reinstated. ARAIM navigation performances using both equal and non-equal allocations are evaluated in the next section.

5 Anticipated H-ARAIM navigation performance

5.1 Predictive integrity risk

To quantify the expected ARAIM navigation performance, an offline analysis is usually carried out. To do this, the integrity risk is predicted prior to the operations. In principle, the predictive integrity risk ${}^{P}P_{HMI}$ needs to characterise all the scenarios that the user may encounter in real time. However, it is not feasible to exactly capture the complex and various operational environments in advance, because the actual satellite geometry may change due to many factors, such as the aircraft banking. Therefore, the evaluation of ${}^{P}P_{HMI}$ depends on the assumptions on the real-time operations.

This work focuses on addressing the impact of SO on ARAIM, so the predictive integrity risk will account for the integrity threat when the user undergoes SO

$${}^{P}P_{HMI} = \sum_{k=0}^{N} P_{HMI|O_k} P_{O_k} \tag{25}$$

$$< \sum_{k=0}^{n} P_{HMI|O_k} P_{O_k} + P_{NM,SO} \tag{26}$$

As suggested by (25), ${}^{P}P_{HMI}$ is a weighted sum of the conditional integrity risk $P_{HMI|O_k}$ under 'O_k'. If the 'equal allocation' approach in Section 4.1 is employed, both the detection and exclusion functions are always implemented regardless of SO. Therefore, $P_{HMI|O_k}$ is identical to ${}^{I}P_{HMI,FDE}$, which can be upper bounded using (7). If the 'non-equal allocation' approach is applied, $P_{HMI|O_k}$ is either equivalent to ${}^{I}P_{HMI,FD}$ or ${}^{I}P_{HMI,FDE}$, depending on whether the receiver is implementing exclusion function under 'O_k'.

5.2 Results

With the theoretical methods being derived in previous sections, this section demonstrates H-ARAIM navigation performance in terms of availability of ${}^{P}P_{HMI} < I_{REQ}$. Dual-frequency baseline GPS/Galileo constellations under nominal simulation conditions are employed for two intended operations: RNP 0.1 and 0.3. The almanac files are downloaded from the link in [9] to provide coarse SV positions, which are sufficient for covariance analysis. The key simulation parameters, which are modified from [9], are listed in Table 3.

To be general and rigorous, the method we developed in this paper captures all the outage scenarios, including dual SO and multiple SO. However, since SO only impacts continuity, it may not be necessary to always account for the simultaneous SO on

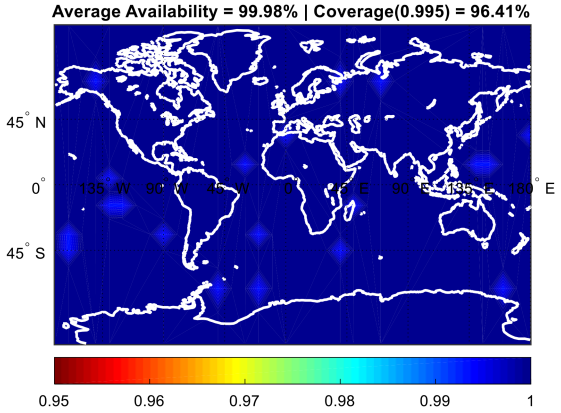

Fig. 4 *H-ARAIM availability of ${}^{p}P_{HMI} < I_{REQ}$ for RNP 0.1 without including the impact of SO*

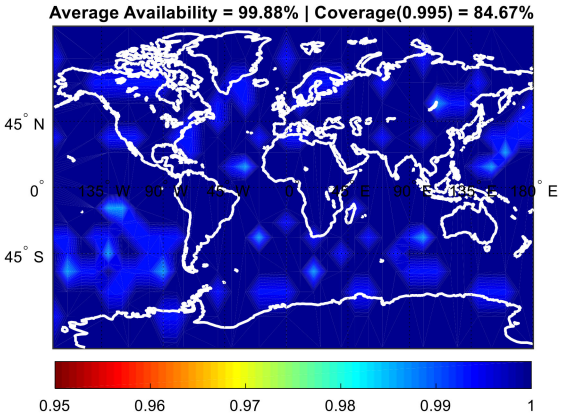

Fig. 5 *H-ARAIM availability of ${}^{p}P_{HMI} < I_{REQ}$ for RNP 0.1 when accounting for single SO (equal allocation)*

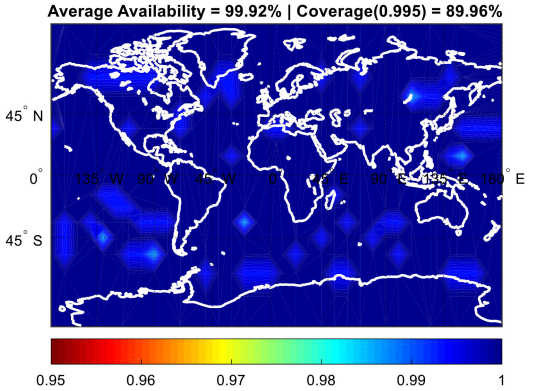

Fig. 6 *H-ARAIM availability of ${}^{p}P_{HMI} < I_{REQ}$ for RNP 0.1 when accounting for single SO (non-equal allocation)*

multiple SVs. Therefore, from the operation perspective, the impact of single SO is of primary interest. That is why two analyses are carried out by (i) only accounting for single SV outages and (ii) rigorously accounting for all the SO modes using (11).

Figs. 4–6 present the H-ARAIM availability of ${}^{p}P_{\mathrm{HMI}} < I_{\mathrm{REQ}}$ under different simulation scenarios. According to Fig. 4, the nominal H-ARAIM FDE algorithm is achieving 96.31% coverage, which reflects the fraction of users in the investigated region that have availability >0.995. Due to impact of SO, the coverage drops to 84.67% using the 'equal allocation' approach introduced in Section 4.1, and to 89.96% using the 'non-equal allocation' approach introduced in Section 4.2.

Table 4 summarises the analyses, and shows coverages for both RNP 0.1 and 0.3. According to the results, high availability can be achieved, which implies the SO does not significantly impact the H-ARAIM navigation performance. As mentioned in prior sections, the performance evaluated using 'non-equal' allocation can be further improved by optimally allocating $P_{\mathrm{alert,REQ}}$, even though it may come at a cost of the computational load.

Table 4 H-ARAIM availability coverages

	Single SO only, %	All SO cases, %
RNP 0.1, equal allocation	84.67	81.11
RNP 0.1, non-equal allocation	89.96	88.97
RNP 0.3, equal allocation	94.81	94.39
RNP 0.3, non-equal allocation	95.54	95.24

6 Conclusion

This paper evaluates the impact of SO on H-ARAIM). A new method to quantify the overall continuity risk is derived. The proposed approach accounts for LOC contributions from both measurement faults and SOs. A method is given to determine FDE threshold ensuring that a predefined continuity requirement can be achieved. Two methods to allocate the continuity budget across SO scenarios are described. In addition, an integrity risk equation is derived from capturing the risk of HMI under SO conditions. This equation was implemented for H-ARAIM coverage performance prediction. In performance analyses, coverage results obtained using new method are compared to the ones without accounting for SO. Results show that SO only cause coverage to decrease by a small amount, which indicates the H-ARAIM navigation performance will not be significantly impacted by SO.

7 Acknowledgments

The authors thank the Federal Aviation Administration (FAA) for sponsoring this work (grant number DTFAWA-16-X-00004). However, the views and opinions expressed in this paper are those of the authors and do not necessarily reflect those of any other organisation or person.

8 References

[1] Pervan, B.: 'Navigation integrity for aircraft precision landing using the global positioning system'. PhD. Dissertation, Department of Aeronautics and Astronautics, Stanford University, Stanford, CA, 1996

[2] Lee, Y.C.: 'Analysis of range and position comparison methods as a means to provide GPS integrity in the user receiver'. Proc. of the 42nd Annual Meeting of The Institute of Navigation, Seattle, WA, 1986, pp. 1–4

[3] Parkinson, B.W., Axelrad, P.: 'Autonomous GPS integrity monitoring using the pseudorange residual', *Navig., J. Inst. Navig.*, 1988, **35**, (2), pp. 255–274

[4] RTCA Special Committee 159: 'Minimum operational performance standards for airborne supplemental navigation equipment using global positioning system (GPS)', RTCA/DO-208, July 1991

[5] Joerger, M., Chan, F.-C., Pervan, B.: 'Solution separation versus residual-based RAIM', *Navig., J. Inst. Navig.*, 2014, **61**, (4), pp. 273–291

[6] Phase II of the GNSS Evolutionary Architecture Study, February 2010

[7] EU-U.S. Cooperation on Satellite Navigation, Working Group C: 'ARAIM technical subgroup interim report', Issue 1.0, 19 December 2012

[8] Blanch, J., Walter, T., Enge, P., *et al.*: 'Baseline advanced RAIM user algorithm and possible improvements', *IEEE Trans. Aerosp. Electron. Syst.*, 2015, **51**, (1), pp. 713–732

[9] EU-U.S. Cooperation on Satellite Navigation, Working Group C: 'ARAIM technical subgroup milestone 3 report', 25 February 2016

[10] ICAO, Annex 10, aeronautical telecommunications, volume 1 (Radio Navigation Aids), Amendment 84, published 20 July 2009, effective 19 November 2009

[11] Blanch, J., Walter, T., Enge, P., *et al.*: 'A simple position estimator that improves advanced RAIM performance', *IEEE Trans. Aerosp. Electron. Syst.*, 2015, **51**, (3), pp. 2485–2489

[12] Joerger, M., Stevanovic, S., Langel, S., *et al.*: 'Integrity risk minimisation in RAIM part 1: optimal detector design', *J. Navig.*, 2016, **69**, (3), pp. 449–467

[13] Joerger, M., Langel, S., Pervan, B.: 'Integrity risk minimisation in RAIM part 2: optimal estimator design', *J. Navig.*, 2016, **69**, (4), pp. 709–728

[14] Blanch, J., Walter, T., Enge, P.: 'RAIM with optimal integrity and continuity allocations under multiple failures', *IEEE Trans. Aerosp. Electron. Syst.*, 2009, **46**, (3), pp. 1235–1247

[15] Lee, Y., McLaughlin, M.: 'Feasibility analysis of RAIM to provide LPV-200 approaches with future GPS'. Proc. of the 20th Int. Technical Meeting of the Satellite Division of The Institute of Navigation, Fort Worth, TX, September 2007, pp. 2898–2910

[16] Zhai, Y., Joerger, M., Pervan, B.: 'Continuity and availability in dual-frequency multi-constellation ARAIM'. Proc. of the 28th Int. Technical

Meeting of The Satellite Division of the Institute of Navigation, Tampa, Florida, September 2015, pp. 664–674
[17] Zhai, Y., Joerger, M., Pervan, B.: 'Bounding continuity risk in H-ARAIM FDE'. Proc. of the ION 2017 Pacific PNT Meeting, Honolulu, Hawaii, May 2017, pp. 20–35
[18] Zhai, Y., Joerger, M., Pervan, B.: 'Fault exclusion in multi-constellation global navigation satellite systems', *J. Navig.*, 2018, **71**, (6), pp. 1281–1298, doi: 10.1017/S0373463318000383
[19] Zhai, Y., Joerger, M., Pervan, B.: 'H-ARAIM exclusion: requirements and performance'. Proc. of the 29th Int. Technical Meeting of The Satellite Division of the Institute of Navigation, Portland, Oregon, September 2016, pp. 1713–1725
[20] RTCA Special Committee 159: 'Minimum aviation system performance standards for the local area augmentation system (LAAS)', RTCA/DO-245, 2004, Appendix D
[21] Walter, T., Blanch, J., Joerger, M., *et al.*: 'Determination of fault probabilities for ARAIM'. Proc. of IEEE/ION PLANS 2016, Savannah, GA, April 2016, pp. 451–461
[22] Zhai, Y.: 'Ensuring navigation integrity and continuity using multi-constellation GNSS'. PhD. Dissertation, Illinois Institute of Technology, Chicago, IL, 2018
[23] Joerger, M.: 'ARAIM continuity assertions', E.U.-U.S. ARAIM Working Group Report, 2018
[24] FAA-E-2892d, system specification for the wide area augmentation system, 28 March 2012
[25] RTCA Special Committee 159: 'Minimum operational performance standards for global positioning system/wide area augmentation system airborne equipment'. Document No. RTCA/DO-229D, Washington, DC, 2006
[26] Lee, Y., Dyke, V.K., Decleene, B., *et al.*: 'Summary of RTCA SC-159 GPS integrity working group activities', *Navig., J. Inst. Navig.*, 1996, **43**, (3), pp. 307–362
[27] Assistant Secretary of Defense for Command, Control, Communications and Intelligence: 'Global positioning system standard positioning service performance standard'. Washington, DC, 2008
[28] Pullen, S., Enge, P.: 'Using outage history to exclude high-risk satellites from GBAS corrections', *Navig., J. Inst. Navig.*, 2013, **60**, (1), pp. 41–51
[29] Blanch, J.: 'Continuity requirements for H-ARAIM and a proposed baseline approach for exclusion'. Presented to ARAIM Working Group, Toulouse, April 2017

9 Appendix

This appendix drives the equations to compute the FDE thresholds when $P_{\text{alert,REQ}}$ are non-equally allocated over SO conditions. Using mathematical terms, (16) is rewritten and bounded by

$$P_{\text{FANE,OF}} < P\left(\bigcup_{d=1}^{h_0} |q_d| > T_{d|O_0} \,|\, H_0, O_0\right) P_{H_0} P_{O_0} \tag{27}$$

$$< \sum_{d=1}^{h_0} P\left(|q_d| > T_{d|O_0} \;\middle|\; H_0, O_0\right) P_{H_0} P_{O_0} \tag{28}$$

By limiting equation (28) using the $P_{\text{FANE,OF,REQ}}$ in Table 2, the detection threshold under OF condition ($T_{d\,|O_0}$) can be computed

$$T_{d|O_0} = Q^{-1}\left\{\frac{P_{\text{FANE,OF,REQ}}}{2P_{H_0} \cdot P_{O_0} \cdot h_0}\right\} \tag{29}$$

$P_{\text{FDNE,OF}}$, which is shown in (18), can be further bounded by

$$P_{\text{FDNE,OF}} - P_{\text{NM,Fault}} P_{O_0} < \sum_{i=1}^{h_0} P\left(\bigcap_{e=1}^{h_0}\left(\bigcup_{l=1}^{s_0} |q_{e,l}| > T_{e,l\,|O_0}\right) |H_i,\ O_0\right) P_{H_i} P_{O_0} \tag{30}$$

$$< \sum_{i=1}^{h_0} P\left(\bigcup_{l=1}^{s_0} |q_{i,l}| > T_{i,l\,|O_0} |H_i,\ O_0\right) P_{H_i} P_{O_0} \tag{31}$$

$$< \sum_{i=1}^{h_0} \sum_{l=1}^{s_0} P\left(|q_{i,l}| > T_{i,l\,|O_0} |H_i, O_0\right) P_{H_i} P_{O_0} \tag{32}$$

The bound used in the transition from equation (30) to (31) is worth clarifying, where only one exclusion option, associated with the correct fault hypothesis is considered, that is, $e = i$. Since the actual fault is excluded, the exclusion statistics in equations (31) and (32) are FF. In this work, we use an even allocation of $P_{\text{FDNE,OF,REQ}} - P_{\text{NM,Fault}} P_{O_0}$ over all the hypotheses. Therefore

$$T_{i,l\,|O_0} = Q^{-1}\left\{\frac{P_{\text{FDNE,OF,REQ}} - P_{\text{NM,Fault}} P_{O_0}}{2P_{H_i} \cdot P_{O_0} \cdot h_0 \cdot s_0}\right\} \tag{33}$$

A similar approach to OF case can be applied to compute FDE thresholds after a SO has occurred, except the prior probabilities of SO are much smaller than P_{O_0}. $P_{\text{FANE,SO}}$ can be rewritten and bounded as

$$P_{\text{FANE,SO}} - P_{H_0} P_{\text{NM,SO}} < \sum_{k=1}^{n} P\left(\bigcup_{d=1}^{h_k} |q_d| > T_{d\,|O_k} |H_0,\ O_k\right) P_{H_0} P_{O_k} \tag{34}$$

$$< \sum_{k=1}^{n} \sum_{d=1}^{h_k} P\left(|q_d| > T_{d\,|O_k}\,|H_0,\ O_k\right) P_{H_0} P_{O_k} \tag{35}$$

By limiting equation (35) using $P_{\text{FANE,SO,REQ}} - P_{H_0} P_{\text{NM,SO}}$, $T_{d|O_k}$ can be solved

$$T_{d|O_k} = Q^{-1}\left\{\frac{P_{\text{FANE,SO,REQ}} - P_{H_0} P_{\text{NM,SO}}}{2P_{H_0} \cdot P_{O_k} \cdot n \cdot h_k}\right\} \tag{36}$$

Finally, $P_{\text{FDNE,SO}}$ is further bounded as follows:

$$P_{\text{FDNE,SO}} - P_{\text{NM,Fault}} P_{\text{NM,SO}} < \sum_{k=1}^{n} \sum_{i=1}^{h_k} P\left(\bigcap_{e=1}^{h_k}\left(\bigcup_{l=1}^{s_k} |q_{e,l}| > T_{e,l\,|O_k}\right) |H_i, O_k\right) P_{H_i} P_{O_k} \tag{37}$$

$$< \sum_{k=1}^{n} \sum_{i=1}^{h_k} P\left(\bigcup_{l=1}^{s_k} |q_{i,l}| > T_{i,l\,|O_k} |H_i, O_k\right) P_{H_i} P_{O_k} \tag{38}$$

$$< \sum_{k=1}^{n} \sum_{i=1}^{h_k} \sum_{l=1}^{s_k} P\left(|q_{i,l}| > T_{i,l\,|O_k}\,|H_i, O_k\right) P_{H_i} P_{O_k} \tag{39}$$

Therefore, the exclusion thresholds under SO conditions $T_{i,l\,|O_k}$ can be computed

$$T_{i,l\,|O_k} = Q^{-1}\left\{\frac{P_{\text{FDNE,SO,REQ}} - P_{\text{NM,Fault}} P_{\text{NM,SO}}}{2P_{H_i} \cdot P_{O_k} \cdot n \cdot h_k \cdot s_k}\right\} \tag{40}$$